

This version of the article has been accepted for publication, after peer review (when applicable) and is subject to Springer Nature's AM terms of use, but is not the Version of Record and does not reflect post-acceptance improvements, or any corrections. The Version of Record is available online at: <https://doi.org/10.1007/s00430-014-0343-4>

Boros-Majewska J., Salewska N., Borowski E., Milewski S., Malic S., Wei X., Hayes A., Wilson M., Williams D., Novel Nystatin A₁ derivatives exhibiting low host cell toxicity and antifungal activity in an *in vitro* model of oral candidosis, *MEDICAL MICROBIOLOGY AND IMMUNOLOGY*, Vol. 203, Iss. 5 (2014), pp. 341-355

Novel Nystatin A₁ derivatives exhibiting low host cell toxicity are effective in an *in vitro* model of oral candidosis

Joanna Boros-Majewska, Natalia Salewska, Edward Borowski, Sławomir Milewski, Sladjana Malic, Xiao-Qing Wei, Anthony J. Hayes, Melanie J. Wilson, David W. Williams

J. Boros-Majewska^{1,2}, E. Borowski^{1,2}, S. Milewski¹

¹Department of Pharmaceutical Technology and Biochemistry, Gdansk University of Technology (GUT), 11/12 Narutowicza Street, 80-233 Gdansk, Poland

²BLIRT S.A., 3/1.38 Trzy Lipy Street, 80-172 Gdansk, Poland

N. Salewska^{2,3}

³Department of Organic Chemistry, Gdansk University of Technology, 11/12 Narutowicza Street, 80-233 Gdansk, Poland

S. Malic⁴,

⁴School of Healthcare Sciences, Manchester Metropolitan University, Manchester, M1 5GD, UK

X. Wei, M. J. Wilson, D. W. Williams⁵

⁵Tissue Engineering and Reparative Dentistry, School of Dentistry, Cardiff University, Heath Park, Cardiff, CF14 4XY, UK

Corresponding author: David W. Williams

E-mail: WilliamsDD@cardiff.ac.uk

Telephone: +44 (0)29 2074 2548

Telefax: +44 (0)29 2074 6489

A. J. Hayes⁶

⁶Bioimaging Unit, School of Biosciences, Cardiff University, Park Place, Cardiff, CF10 3US, UK

Abstract

Opportunistic oral infections caused by *Candida albicans*, have become a frequent problem in immunocompromised patients. Management of such infections is limited, due to the low number of antifungal drugs available, their relatively high toxicity and the emergence of antifungal resistance. Given these issues, our investigations have focused on novel derivatives of the antifungal antibiotic Nystatin A₁, generated by modifications at the amino group of this molecule. The aims of this study were to evaluate the antifungal effectiveness and host cell toxicity of these new compounds using an *in vitro* model of oral candidosis based on a reconstituted human oral epithelium (RHOE). Initial studies employing broth microdilution, revealed that against planktonic *C. albicans*, Nystatin A₁ had lower minimal inhibitory concentration (MIC); however, Nystatin A₁ was also markedly more toxic against human keratinocyte cells (HaCaT), compared with novel derivatives. Interestingly, using live/dead staining to assess *C. albicans* and tissue cell viability after RHOE infection, Nystatin A₁ derivatives were more active against *Candida* with lower toxicity to epithelial cells than the parent drug. Lactate dehydrogenase activity released by the RHOE also indicated a four-fold reduction in tissue damage when certain Nystatin derivatives were used, compared with Nystatin A₁. Furthermore, compared with Nystatin A₁, colonization of the oral epithelium by *C. albicans* was notably reduced by the new polyenes. In the absence of antifungal agents, confocal laser scanning microscopy showed that *C. albicans* extensively invaded the RHOE. However, the presence of the novel derivatives greatly reduced or totally prevented this fungal invasion.

Keywords *Candida albicans*; antifungals; Nystatin A₁; candidosis; oral infections; cytotoxicity

Introduction

During recent decades, the number of people with immune system disorders has increased markedly. Such individuals include those who are diabetic, patients with haematological malignancies such as acute leukaemia, cancer patients who are exposed to high doses of chemotherapy or radiation therapy, transplantation surgery patients and HIV-positive persons [1]. According to World Health Organization reports, the number of HIV infected humans in 2008 reached 33.4 million [2]. In the same year, the number of cancer cases amounted to 20 million [3], whilst, latest data show that 347 million people suffer from diabetes mellitus [4]. Associated with the chronic problems of these immunocompromised individuals, are the added complications of opportunistic infections, of which oral candidosis (OC) is extremely prevalent [5-7].

In addition to the above, there are other debilitating factors that enhance the risk of *Candida* infection. For example, an increased prevalence of oral candidosis is evident amongst elderly

individuals, pregnant women and newborn babies, as well as in people with some form of nutritional deficit, such as iron or vitamin B12 deficiency [8, 9]. Moreover, *Candida* overgrowth is often promoted by excessive use of medications, especially broad-spectrum antibiotics, which disturb the natural community of the bacterial microflora, and corticosteroids, which can suppress nonspecific inflammatory responses. Apart from systemic risks, local predisposing factors include an insufficient degree or absence of oral hygiene, tobacco smoking, wearing of dental prostheses, a diet rich in carbohydrates and hyposalivation [8, 9].

The principal causative agent of oral candidosis is *Candida albicans*. This polymorphic fungus frequently colonises the oral cavity and digestive tract surfaces of humans as a harmless commensal. However, as mentioned above, when individuals become debilitated *C. albicans* overgrowth can arise, resulting in infection [10, 11].

Clinically, in its primary form, oral candidosis presents on the mucosa of the pharynx and oesophagus.

Meanwhile, secondary lesions can lead to symptoms of systemic or disseminated mycoses. Primary oral candidosis can be widespread and is divided into three clinically distinct types. Pseudomembranous and erythematous candidosis manifest as either acute or chronic variants, whilst hyperplastic infection develops only as a chronic condition. Each type of infection has a different clinical presentation, occurs in specific groups of patients and often requires different approaches of treatment [12, 13].

Currently, two main classes of antifungal drugs are used in the management of oral candidosis, namely, azole and polyene agents [12-14]. Their antifungal action results from the presence of ergosterol, as an essential component of the fungal cell membrane. Azole compounds inhibit the fungal cytochrome P450 (CYP) dependent enzyme, lanosterol 14 α -demethylase, which participates in the ergosterol biosynthesis pathway. As a result, ergosterol depletion and accumulation of improper sterols disturb the correct structure and functioning of the cell membrane and finally inhibit fungal cell growth [13-15].

The majority of azole antifungals, of which fluconazole is the main representative, exhibit a high bioavailability after oral administration. However, through inhibition of the human cytochrome P450 (CYP) enzyme system, azoles can also initiate undesirable drug-drug interactions. These interactions may reduce drug absorption or increase the risk of adverse effects, which are especially dangerous in patients receiving immunosuppressive or cardiovascular therapy [15]. Similarly problematic, is the emergence of *Candida* resistance to azoles, mainly arising due to point mutations in the azole-binding site of α -demethylase and/or by overproduction of multi-drug efflux pumps that are able to actively expel the drug from the fungal cell [16].

In contrast to azole compounds, polyene antibiotics bind to ergosterol directly and form transmembrane channels. These membrane channels significantly increase membrane permeability and cause leakage of cellular contents. Fungicidal action and low incidence of fungal resistance are the

most advantageous features of polyenes. However, despite greater affinity to the fungal sterol, ergosterol, there is a tendency for polyenes to also interact with the human membrane component, cholesterol, and this can lead to numerous side effects [17]. Moreover, low absorption through the gastrointestinal tract creates many difficulties in drug administration and restricts the use of polyenes in oral candidosis to topical applications [12, 17].

Without doubt, current antifungal chemotherapy has a number of key limitations, and the lack of highly effective and selective antifungal drugs to adequately treat the conditions often results in recurrence of *Candida* infections [18]. Consequently, there is an urgent need for the development of novel and advanced antifungal agents that overcome the problems of those currently available. One proposed strategy is rational chemical modification, designed to improve existing properties of native drugs [19-21].

Prior to the present study, efforts had been made to modify the structure of the polyene antibiotic, Nystatin A₁ (Fig. 1) to reduce toxicity and increase water solubility. Previous reports have shown that an amino group of the polyene molecule plays an essential role in membrane interactions, whilst the presence of additional polar functional groups may improve solubility in water [19, 21, 22]. Therefore, novel *N*-substituted derivatives of Nystatin A₁ have been recently synthesized as potential antifungal agents [23].

The aims of our investigations were to assess the effectiveness and toxicity of these novel Nystatin A₁ derivatives using an *in vitro* model of oral candidosis. Antifungal activity against *C. albicans* and cytotoxic effects on a human keratinocyte cell line were initially examined. Subsequently, *Candida* infection of a reconstituted human oral epithelium (RHOE) was successfully developed, and the extent of epithelial cell damage/viability was measured using lactate dehydrogenase activity and live/dead staining. The degree of tissue colonization and profile of tissue invasion by *C. albicans* was analysed using immunofluorescence labeling and confocal laser scanning microscopy (CLSM). *Candida* viability was also determined by live/dead staining and CLSM imaging. The effect on these measured parameters, was determined post treatment with different Nystatin A₁ derivatives and based on these experiments, identification of novel Nystatin A₁ derivative(s) with appropriate function and reduced toxicity were made.

Materials and Methods

Candida albicans and reconstituted human oral epithelium

All experiments were performed using the reference strain of *C. albicans* ATCC 10231. Initial cytotoxic effects of antifungal drugs were tested using a human keratinocyte cell line (HaCaT) from the collection of the School of Dentistry, Cardiff University (UK). A commercially available reconstituted human oral epithelium (RHOE, SkinEthic Laboratories; Nice, France) that had

previously been established as an *in vitro* tissue model of oral candidosis [24, 25] was utilised in these infection studies.

Antifungal compounds

Nystatin A₁ (Nys) was obtained from Sigma Aldrich (Poole, UK) and the novel Nystatin A₁ derivatives were designed and synthesised at BLIRT S.A. Company, Gdansk (Poland) [23] and the Department of Organic Chemistry and Department of Pharmaceutical Technology & Biochemistry at GUT (Poland). All derivatives were divided into classes depending on the functional group attached to the nitrogen atom in the native macrolide structure and selected representatives (Nys1, Nys2, Nys4, Nys5, Nys6, Nys7, Nys8) were the focus of these studies. These derivatives form water-soluble salts. N-fructosyl Nystatin A₁ (Nys3) [26] was used as a reference derivative of Nystatin A₁. Stock solutions of Nystatin A₁ and its derivatives were prepared in dimethyl sulfoxide (DMSO; Sigma-Aldrich, Poole, UK). As the native Nystatin A₁ is water-insoluble and requires the use of DMSO to make the stock solution, the antibiotic derivatives were used not in the form of their water-soluble salts, to ensure the same conditions for testing of all compounds.

Antifungal susceptibility testing

In vitro antifungal activity of Nystatin A₁ and *N*-substituted derivatives was initially measured based on the broth microdilution method of the Clinical and Laboratory Standards Institute (CLSI, formerly NCCLS), [27] with the exception that a final inoculum density of 1×10^4 cells ml⁻¹ was used. The Minimal Inhibitory Concentration (MIC) was determined for *C. albicans* using RPMI-1640 medium (with L-glutamine and phenol red, without sodium bicarbonate, Sigma-Aldrich, Poole, UK) buffered to pH 7.0 with MOPS buffer ([3-(*N*-morpholino) propanesulfonic acid], Sigma-Aldrich). Appropriate solutions of studied compounds previously prepared in DMSO were diluted in the RPMI-1640 medium to give final concentration ranges of 0.03125-16 µg ml⁻¹ for Nystatin A₁ and 0.250-128 µg ml⁻¹ for the new derivatives. The final DMSO concentration in each well was 1% (v/v). Microtitre plates were incubated at 30°C and optical absorbance (OD_{531nm}) recorded after 24 h with a plate reader (VICTOR³™ Multilabel Counter, Perkin Elmer, Massachusetts, USA). The MIC was defined as the lowest compound concentration that provided complete inhibition of visible growth. A half maximal inhibitory concentrations (IC_{50-C}) were also estimated by preparing graphs from measured optical density (OD_{531nm}) values as a function of drug concentration and fitting these data to the sigmoidal dose-response equations using Origin Pro 8.1 software (OriginLab Corporation, Northampton, USA). Susceptibility tests were repeated on three separate occasions.

Cytotoxicity studies of antifungal compounds

The *in vitro* cytotoxic effects of Nystatin A₁ and the novel derivatives on human cells was undertaken using a keratinocyte cell line (HaCaT) in DMEM medium containing high glucose concentration and

L-glutamine (Lonza Group Ltd., Basel, Switzerland) supplemented with 10% Fetal Bovine Serum (FBS) and penicillin/streptomycin (100 U ml⁻¹ and 100 µg ml⁻¹, respectively, Lonza Group Ltd.). After washing twice with phosphate-buffered saline (PBS, pH=7.0), HaCaT cells were harvested using trypsin-EDTA solution (Lonza Group Ltd.) and the number of cells enumerated with a haemocytometer before adjustment to a density of 2×10⁶ cells ml⁻¹ in DMEM medium. Serial doubling dilutions of the keratinocyte cell suspension was performed in a 96-well tissue culture plate (Sarstedt, Nümbrecht, Germany) which also included a growth control commencing at 1×10⁵ cells ml⁻¹.

For drug testing, 100 µl of 2×10⁴ cells per well were seeded in each well with the same volume of appropriately diluted compound in culture medium. The antifungal concentration range was 12.5-300 µg ml⁻¹ and the final DMSO concentration in all microtitre wells was 1% (v/v). Keratinocytes were incubated for 3 days at 37°C in a humidified atmosphere containing 5% CO₂. After incubation, cell viability was determined using the Cell Counting Kit-8 (Sigma-Aldrich). This colorimetric assay was based on the reduction of water-soluble tetrazolium salt to a coloured product – formazan by active dehydrogenases of viable cells. The amount of water-soluble formazan dye was therefore directly proportional to the number of living cells. After 3 days, 100 µl of the removed culture medium was replaced by 100 µl of 10-fold diluted CCK-8 reagent. Incubation was continued for another 4 h and the absorbance was then measured at 450_{nm} in a plate reader (FLUOstar Omega; BMG LABTECH GmbH, Ortenberg, Germany). Cell viability was evaluated by plotting optical density values (OD₄₅₀) as a function of drug concentration and the IC₅₀-H (half maximal inhibitory concentration) value calculated by fitting the results to the sigmoidal dose-response equations in the Origin Pro 8.1 software. For each compound, the experiments were performed in triplicate.

***In vitro* tissue model of oral candidosis treated with antifungals**

To further examine antifungal effectiveness of the compounds, an *in vitro* tissue model of oral candidosis was utilised. For this purpose, a reconstituted human oral epithelium (RHOE) and *C. albicans* were used. Before each experiment, *C. albicans* was cultured on Sabouraud Dextrose Agar (Oxoid Ltd., Hampshire, UK) for 48 h at 30°C and a portion of colony growth then re-suspended and incubated in Yeast Nitrogen Base medium (0.67% YNB without amino acids; BD Diagnostics, Cowley, UK) supplemented with 0.5% glucose (Merck, Darmstadt, Germany) for 12 h with gentle agitation at 37°C. Cells were then harvested by centrifugation, washed three times with sterile phosphate-buffered saline (PBS, pH=7.0) before resuspension in fresh PBS.

To establish the *in vitro* tissue infection, *Candida* yeast were enumerated in an Improved Neubauer haemocytometer and adjusted to a final concentration of 2×10⁶ cells ml⁻¹ in Maintenance Medium (SkinEthic Laboratories, Nice, France), used for RHOE cultivation. Finally, RHOE tissue inserts (0.5 cm², age day 5) were transferred to a sterile 24-well tissue culture plate (Sarstedt, Nümbrecht, Germany) and inoculated with 1 ml of standardized yeast suspension (2×10⁶ cells ml⁻¹). A control of non-infected tissue with 1 ml of medium devoid of *Candida* was also prepared. All tissues were

incubated for 6 h at 37°C in a humidified atmosphere with 5% CO₂. Supernatants were then removed, and 1 ml of the antifungal compound solutions in Maintenance Medium added to the tissue surfaces. Experiments were performed at a total drug concentration of 150 µg ml⁻¹ in 1% (v/v) DMSO. Maximal fungal infection controls were obtained by incubation of RHOE tissue with Maintenance medium incorporating 1% (v/v) DMSO. Similarly, non-infected tissue controls, utilised replacement of supernatant with fresh medium containing 1% DMSO. After overnight incubation, supernatant was collected for lactate dehydrogenase measurement and the tissues were rinsed with phosphate-buffered saline. All inserts were divided in half, with one portion used for live/dead staining and the other portion prepared for CLSM. All experiments were performed on five separate occasions.

Live/dead assay of infected tissues

Determination of *C. albicans* viability after antifungal treatment was based on the use of live/dead staining. Portions of fresh (*i.e.* not fixed) RHOE tissues post-infection, were placed on to microscope slides and 100 µl of a fluorescent dye mixture (25 µM Syto9 and 15 µM propidium iodide, Molecular Probes-Invitrogen, Paisley, UK) directly added. The green fluorescing nucleic acid dye, Syto9, was used to stain both live and dead cells, whilst the red fluorescing dye, propidium iodide, was used to stain only dead cells. Samples were incubated for 30 min at 37°C in the dark, transferred to clean slides and overlaid with Vectashield Mounting Medium (H-1000, Vector Laboratories, Inc., Burlingame, CA) for prevention of dye photo bleaching. Stained tissues were observed by CLSM using a Leica TCS SP2 AOBS spectral confocal microscope (Leica Microsystems GmbH, Wetzlar, Germany). Tissue halves were scanned through a 15-µm depth with a ×40 objective lens at a Z-step of approximately 0.5 µm. To eliminate spectral bleed-through between fluorescent probes, sections were scanned using appropriate settings for sequential fluorescence recordings of Syto9 (ex/em max: 480/500_{nm}) and propidium iodide (ex/em max: 490/635_{nm}). Images were presented as maximum intensity type reconstructions and were used for fluorescent areas enumerations. The experiments were performed in triplicate.

Live/dead cell determination

The effect of the tested compounds on both *Candida albicans* and RHOE cell viability was determined from confocal microscopy images. Total area of green and red fluorescence in relation to each image area was calculated using an image analysis program– ImageJ 1.46r (Wayne Rasband, National Institute of Health, USA). Firstly, the image was divided into green and red channels and the function of threshold intensity was utilised. Subsequently, the green and red area measurements for both cell types (*Candida* and epithelial cells) were made with the use of the ‘Analyze Particles’ ImageJ tool. All calculations were made for three separate images. For easier comparison of all data, green and red fluorescent areas for each type of cell in a single image were summed, assumed as a total and the

percentage of live and dead cells computed separately for *C. albicans* and epithelial cells. Results were presented as a mean of three independent images.

Tissue sections preparation for CLSM

Tissue colonisation and invasion by *C. albicans* in the presence and absence of antifungal agents was determined by CLSM after immunofluorescent labeling of tissue sections. For section preparation, infected tissues were fixed in formalin for 24 h at 4°C and embedded in paraffin wax. Tissues sections (20 µm) were generated and placed on Histobond + coated microscope slides (Raymond A Lamb, East Sussex, UK). Sections were then de-waxed, re-hydrated and heated twice for 5 min at 95°C in 10 mM citrate buffer (pH=6.0) to break formalin cross-links and expose target antigens. After cooling, sections were washed in water (×3 for 2 min) and potential non-specific binding sites blocked with normal goat serum (Sigma-Aldrich) at a 1:20 dilution for 30 min at room temperature. Subsequently, sections were incubated overnight at 4°C with a mouse monoclonal IgG pan-cytokeratin primary antibody at 2 µg ml⁻¹ (Santa Cruz Biotechnology, Inc., Dallas, USA). Tissue sections were then washed in phosphate buffered saline (PBS; ×2 for 5 min) and labeled with Alexa Fluor 488 goat anti-mouse IgG secondary antibody (5 µg ml⁻¹; Molecular Probes-Invitrogen, Paisley, UK) for 35 min at room temperature. After washing, samples were treated with 25 µg ml⁻¹ Concanavalin A lectin conjugated with Alexa Fluor 594 (Molecular Probes-Invitrogen) for 20 min and then stained with Hoechst 33258 dye (2 µg ml⁻¹; Sigma-Aldrich) for another 30 min at room temperature. All antibodies and dye solutions were made up in PBS containing 0.1% Tween 20 (Sigma-Aldrich).

Stained sections were washed, mounted with Vectashield Mounting Medium (H-1000, Vector Laboratories) and analyzed by CLSM using a Leica TCS SP2 AOBS spectral confocal microscope (Leica Microsystems GmbH). Sections were scanned sequentially through their depth using appropriate scan settings for sequential fluorescence recording of Alexa 488 (ex/em max: 495/519_{nm}), Alexa 594 (ex/em max: 590/617_{nm}) and Hoechst 33258 (ex/em max: 352/461_{nm}) as described previously. Images were presented as maximum intensity reconstructions. *Candida albicans* were represented by red Alexa 594 fluorescence, keratinocytes by green Alexa 488 fluorescence and cell nuclei by blue Hoechst 33258 fluorescence. The experiments were performed in five replicates.

For precise determination of the effect of tested compounds on the epithelial colonisation by *Candida* strain, the thickness of fungal layers on RHOE sections were measured using CLSM images. Calculations were made with the ImageJ 1.46r program by dividing the area surface by the width of the *Candida* layer. Results were presented diagrammatically as a mean of three separate images.

Measurement of lactate dehydrogenase activity

The extracellular activity of lactate dehydrogenase (LDH) released from epithelial cells was monitored as an indicator of tissue cell damage. Enzyme activity was measured from collected culture medium after infection of RHOE tissues with *C. albicans* ATCC 10231 and treatment with antifungal drugs

dissolved in DMSO, or RHOE in the presence of solvent alone. To investigate the effect of compounds on epithelial cells in the absence of *Candida*, controls of uninfected tissues as well as those incubated with 1% (v/v) DMSO or with just 150 $\mu\text{g ml}^{-1}$ of antifungals were also tested. For determination of LDH activity, a CytoTox-ONE Homogeneous Integrity Assay kit (Promega, Madison, USA) was used. The method was based on the formation of a fluorescent product as a result of the coenzyme NADH diminishing during the LDH catalyzed reaction. The intensity of fluorescence was analyzed with a plate reader (FLUOstar Optima, BMG LABTECH GmbH, Ortenberg, Germany) at appropriate excitation 544_{nm} and emission 590_{nm} wavelengths, and was proportional to the number of damaged cells. The LDH activity of culture medium alone was subtracted from LDH activity of tissue samples and results expressed as a cytotoxicity percentage relative to the maximum enzyme release (LDH activity from *Candida* infected, untreated controls). The experiments were performed in five replicates for infected tissues and in duplicate for uninfected ones.

Statistical analysis

Statistical analysis of data was performed using Origin Pro 8.1 software (OriginLab Corporation, Northampton, USA). The results of fluorescent area calculations, LDH release measurements as well as *Candida* biofilm thickness and HaCaT cells viability for Nystatin A₁ and the novel derivatives were compared using a one-way analysis of variance (ANOVA) by applying a Tukey multiple comparisons test. Statistically significant differences were set at $P < 0.05$.

Results

In vitro antifungal and cytotoxic effect of Nystatin A₁ and novel derivatives

The *in vitro* antifungal activity of tested compounds was measured according to the CLSI protocol. The effect of *N*-substituted derivatives and native Nystatin A₁ was determined against *C. albicans* ATCC 10231 and defined by the MIC providing complete inhibition of fungal growth. A half maximal inhibitory concentration (IC_{50-C}, where the latter C defines *Candida*) was also calculated.

Our studies showed that all examined derivatives were active against *Candida*; however, they exhibited somewhat higher MIC values compared with the native drug (Table 1).

Amongst the tested derivatives, good antifungal activity with MIC ranging of 2 $\mu\text{g ml}^{-1}$ was demonstrated by Nys5 with MICs of 4 $\mu\text{g ml}^{-1}$ evident with Nys1, Nys2, Nys7 and Nys8. The similar antifungal effect of these derivatives on *C. albicans* seemed to be independent of the functional group present. According to IC_{50-C} calculations, Nys5 was selected (1.19 $\mu\text{g ml}^{-1}$) as the most potent antifungal Nystatin A₁ derivative. It was also interesting, that some derivatives, namely Nys1 and Nys7, although they represented different types of modifications, were characterised by identical antifungal action, as they both had the same MIC and IC_{50-C} (2.81 $\mu\text{g ml}^{-1}$) values.



To determine cytotoxic effects of Nystatin A₁ and its derivatives, we used a keratinocyte cell line (HaCaT) selected because these cells are the major types within a multilayered human epithelium *in vivo*. The data were presented in the form of IC₅₀ values (IC₅₀-H, where H represents HaCaT) obtained from graphs of cell viability as a function of a drug concentration. The substitution of the amino group in the Nystatin A₁ molecule was beneficial and resulted in a reduced toxicity of new polyene compounds (Table 2). We found that semisynthetic derivatives had no significant effect on the vitality of human keratinocytes up to the concentration of 300 µg ml⁻¹, since it was impossible to calculate the concentration, which inhibits the growth of HaCaT cells at 50%. In contrast, the native Nystatin A₁ displayed high cytotoxicity to keratinocytes with the IC₅₀-H value at the level of 50.82 µg ml⁻¹.

For further investigations of novel Nystatin A₁ derivatives, we selected Nys5, due to it having the lowest IC₅₀ value found in the antifungal activity determination and two other derivatives: Nys1 and Nys7, as representatives of different structural groups.

Viability of *Candida albicans* and epithelial cells in the model of fungal infection

To examine whether novel derivatives had the ability to kill *C. albicans* during *in vitro* RHOE infection and to assess the influence of these agents on epithelial cells viability, an *in vitro* infection model was utilised. For this purpose, we firstly incubated human oral epithelium with *C. albicans* ATCC 10231 for 6 h and then exposed infected tissues to antifungal compounds at the concentration of 150 µg ml⁻¹ for another 16 h. Following this process, tissues were stained using a live/dead assay and visualized by confocal scanning laser microscopy (Fig. 2).

All infected tissues (Fig. 2B-F) were colonised by *C. albicans*. To compare CLSM images, the relative percentage of green and red fluorescent areas were calculated and the overall ratio of live and dead cells determined. The red fluorescent nuclear dye, propidium iodide does not enter into living cells and was therefore used to detect only dead cells. In contrast, Syto9, a green fluorescent nucleic acid dye, stained both live and dead cells.

Compared with the control treated with only 1% (v/v) DMSO, where 99% of *Candida* cells were green (Fig. 2B), both the natural Nystatin A₁ and selected derivatives, namely Nys1, Nys5 and Nys7 resulted in red fluorescence of *C. albicans*, typically observed in cell death. The results showed that the new Nystatin A₁ derivatives were more effective against *Candida* in the tissue infection compared with the native drug alone ($P < 0.05$).

Based on our calculations (Fig. 3A), the most active compound, Nys7, generated an 88.5% area of *Candida* cells with red fluorescence, whilst treatment with Nystatin A₁ resulted in only 35% area of dead cells. Incubation with derivative Nys5 resulted in a 77% area of dead *Candida* compared with 69% with Nys1.

The viability of tissue keratinocytes was also calculated (Fig. 3B). In the drug-free control (infected with *C. albicans*), we found that 99% of infected epithelial cells exhibited red fluorescence. Treatment

with native Nystatin A₁ resulted in a statistical reduction in epithelial cell death compared with the control ($P < 0.05$), however, high levels of red tissue fluorescence amounting to 78% remained evident. Interestingly, treatment using the novel compounds induced significantly lower areas of red (*i.e.* dead) epithelial cells than the parent drug. It was established that both derivatives Nys1 and Nys5 had no impact on viability of human keratinocytes in the *in vitro* model compared with the uninfected tissue control ($P > 0.05$) and almost 90% of these cells remained green (*i.e.* viable) after treatment. Only Nys7 demonstrated some toxic effect, since a 48% area of epithelial cells was deemed to be red.

In conclusion, listed Nystatin A₁ derivatives caused high levels of *Candida* cell death and demonstrated low toxicity to human oral epithelium.

Novel antifungal compounds in inhibiting colonisation and invasion of oral epithelium by *Candida albicans*

Infected tissue treated with antifungals were fixed, sectioned and immunofluorescently labelled to analyse the level of tissue colonisation and invasion by *Candida*. From these studies, the aim was to measure changes in the progress of fungal infection and assess whether differences occurred due to the presence of new antifungal compounds.

Our investigations revealed a high ability of *C. albicans* ATCC 10231 to colonise the surface of the human oral epithelium in the drug-free control. There was a high tendency for *C. albicans* to generate a biofilm-like structure, where most of the fungal cells were in the form of hyphae. Moreover, in the absence of antifungals, the tissue was completely invaded by the fungal elements, with both hyphae (predominantly) and some yeast forms detected even at the base of the epithelium. This resulted in the separation of keratinocytes from the membrane insert base and detachment of the epithelium (Fig. 4). Compared with uninfected controls, areas of vacuolation in the tissue structure could also be seen as further evidence of tissue damage.

The action of antifungal compounds significantly inhibited the progress of RHOE infection (Fig. 5). After treatment with native Nystatin A₁, *Candida* was still seen to colonise the surface of the epithelium, but penetration into the tissue was not observed. The fungal layer was two-fold thinner than in the control of solvent alone (1% v/v DMSO; 100.1 μm biofilm thickness; Fig. 6), however *Candida* hyphae were still tightly clustered (Fig. 5B).

Treatment with compound Nys1 did not entirely prevent *C. albicans* invasion of the RHOE (Table 3), although only the upper layers of the epithelium were invaded. Within the tissue, the presence of both hyphae and yeast was observed (Fig. 5C). It was also evident that fungal cells were not organised within a typical biofilm-like form, as noted with the Nystatin A₁ and two other derivatives. In contrast, the stratified growth of *Candida* appeared to be retarded and this resulted in the greatest decrease in the area (24.7 μm thick) occupied by the fungal cells on the epithelium surface, when comparing all the tested compounds (Fig. 6).

In the case of the Nys5 derivative treated oral epithelium, the presence of an approximately 35 μm thin biofilm formed by *Candida* cells on the tissue surface was detected. However, the *Candida* had not invaded the oral epithelium, implying a similar effect of this novel Nystatin derivative to the native drug. Furthermore, fungal colonisation of the RHOE was less extensive compared with the Nystatin A₁ treated tissue, where the *Candida* layer measured 49.4 μm and the structure of the biofilm appeared less densely organised (Fig. 5D).

After treatment with Nys7, the RHOE was covered by thin (31.6 μm) and poorly compacted layer of fungal cells, predominantly in hyphal form, similar to that seen in the tissue treated with Nys5. A few *Candida* were able to invade through the epithelium (Fig. 5E), but this level of invasion was less noticeable compared to the tissue treated with Nys1.

Finally, detachment of the tissue base from keratinocytes layers did not occur under the influence of the antifungal agents.

Based on these results, Nys5 and Nys7 were deemed the most effective antifungals, due to the fact they considerably inhibited the ability of *Candida* to colonize and invade the oral epithelium.

Effect of Nystatin A₁ derivatives on the release of lactate dehydrogenase from infected tissues

Activity of LDH released by the RHOE after *Candida* infection was measured to determine the extent of tissue damage induced by *Candida* in the presence and absence of antifungal compounds (Fig. 7). *Candida albicans* ATCC 10231 induced the maximal level of LDH activity, when the tissue was incubated with solvent alone (1% v/v DMSO). Exposure of uninfected tissue to 1% (v/v) DMSO resulted in LDH activity below 5%, showing that it was the fungal infection that was responsible for the epithelium damage. Nystatin A₁ induced release of LDH from *Candida* infected tissue at the level of 22%, however this was not statistically different from the enzyme activity level of uninfected and Nystatin A₁ treated RHOE (20%; $P > 0.05$).

Novel Nystatin A₁ derivatives reduced LDH activity 4-fold compared with the native compound. In the presence of these new polyenes, the extent of LDH activity was comparable to *Candida* uninfected RHOE tissues and no significant ($P > 0.05$) difference in LDH activity was evident for RHOE treated with the different compounds. Although, LDH activity levels for RHOE treated with the Nystatin A₁ derivatives were different from untreated and uninfected tissue control ($P < 0.05$), they were statistically the same as the uninfected tissue treated only with medium at 1% (v/v) DMSO ($P > 0.05$).

Discussion

Since oral candidosis is a commonly encountered opportunistic fungal disease associated with a variety of symptoms including inflammation and hypertrophy of the oral mucosa and an enhanced possibility of *Candida* dissemination into the other organs, effective methods to combat oral candidosis are required. Amongst the limited armamentarium of drugs for the management of oral



fungal infections, the polyene antibiotics have historically been the most extensively used, and have significant antifungal activity with low incidences of fungal resistance [17].

Polyene antifungals are secondary metabolites produced by *Streptomyces* soil bacteria and consist of a macrolactone ring with a range of conjugated double bonds (3 to 8) and several hydroxyl groups. The lactone core is connected by a glycoside bond with an amino sugar moiety, namely mycosamine, and includes a hemiketal fragment with a carboxylic acid group [28]. The action of polyene compounds is related to the formation of ion channels in fungal membranes rich in ergosterol; however interaction, albeit to a lesser extent, also occurs in mammalian membranes containing cholesterol. Within this group, Nystatin A₁ (Fig. 1) is a leading member for the treatment of oral candidosis and for prevention in patients with a high risk of infections recurrence [12, 13, 17]. Unfortunately, due to toxic side effects after parenteral use, e.g. sclerosing of veins, chills and fever [29], as well as poor oral distribution associated with low water solubility, Nystatin A₁ may be only administrated in the form of topical preparations. Even then, some formulations like suspensions or rinses have reduced efficiency because of saliva dilution and a cleaning action of the oral cavity. Consequently, the effective drug concentration and a sufficient duration of contact time with the oral mucosa may not be achieved, leading to a therapeutic failure [12].

In recent years, considerable effort has been made to circumvent the undesirable features of polyene compounds. These studies have involved production of new antibiotic formulations, genetic manipulation of biosynthetic products and chemical modification of natural drugs. Two Nystatin A₁ formulations, as liposomal and intralipid, that reduce drug toxicity have subsequently been developed [29, 30]. Moreover, clinical trials of liposomal Nystatin A₁ have been completed [31], although such products are known as very expensive for routine antifungal treatment [32]. Meanwhile, the intralipid formulation seems to be a promising, low-cost counterpart, however this remains in the process of testing [33, 34].

Genetic engineering methods are based on manipulation of polyene biosynthetic genes in *Streptomyces* species. During these investigations several new Nystatin-like polyenes have been discovered, with a few of them characterised with better solubility in water and lower toxicity [35], e.g. Nystatin A₁ heptaene S44HP, described by Bruheim et al. [36]. Nevertheless, biosynthetic and genetic engineering techniques tend to be time-consuming and in many cases, result in limited yields of fermentation products [37]. Chemical modification of antibiotic structure appears to be amongst the quickest and most cost effective means to design new improved polyene antifungals. Therefore, a number of polyenes derivatives have been synthesised and some of them have preferable selective toxicity parameters [38-40]. However, previous efforts have largely focused on Amphotericin B, a polyene predominantly used in the treatment of systemic mycoses [41].

Based on the above information, our research has focused on Nystatin A₁, noting that relatively little had been undertaken on to chemically improve this polyene antibiotic. As a result, we present novel Nystatin A₁ derivatives, modified at the amino group, as low toxic and efficient antifungal

compounds for use in combating oral *Candida* infection. In this present study, we have used these agents, for the first time, to treat *in vitro* *Candida* infections of RHOE. Due to the similarity of this tissue model to *in vivo* conditions, it offers a potential alternative to animal research models [25, 42] in assessing compound performance and generates more reliable data than traditional *in vitro* approaches on the behavior of novel agents in the oral cavity environment.

Preliminarily, *in vitro* antifungal activity against *C. albicans* and cytotoxicity on human keratinocyte cells (HaCaT), of the novel compounds were examined separately (Table 1, 2). Both MIC and IC₅₀-C values obtained for Nystatin A₁ were comparable with results of other researchers [43, 44]. Investigations showed that although derivatisation of Nystatin A₁ had no apparent increased antifungal action *in vitro*, there was a significant reduction in the toxicity level of the new compounds. To highlight the latter, compared with Nystatin A₁, the semisynthetic derivatives displayed several-fold reduced toxic effects on HaCaT cells (IC₅₀-H 50.82 vs. >300 µg ml⁻¹). Our findings indicated that the Nystatin A₁ substitution at the nitrogen atom of amino sugar residue with a ‘bulky’ moiety, played an essential role for the reduction of mammalian toxicity of this drug. Previously, similar observations were described for Amphotericin B by Borowski and coworkers [45, 46], who showed that introduction of a large substituent at the amino group generated a sterical hindrance, which decreased the ability of the antibiotic to form lethal channels in cholesterol containing membranes, however still enabled to maintain a good affinity for ergosterol rich ones. Our initial results prompted us to undertake this current research further.

Interaction of *Candida* with the oral epithelium includes attachment and colonisation, invasion and tissue damage which are all important stages during the progress of infection [10, 11, 47]. In this context, we used a tissue model of *Candida* infection to examine how the novel compounds influenced these processes and whether they were able to inhibit the development of oral candidosis. Due to the poor absorption of polyenes into the tissues [12, 13, 17] and based on cytotoxicity results derived to HaCaT cell line, in our experiments we decided to investigate compounds at relatively high concentrations (150 µg ml⁻¹).

For determination of the viability of *Candida* and epithelial tissue cells after the RHOE infection, we successfully used a live/dead assay, allowing clear distinct differentiation of the viable and dead cell populations of both types (Fig. 2). The studies revealed that Nystatin A₁ derivatives were highly effective in the *in vitro* model of oral candidosis. Importantly, novel compounds induced a high extent of *Candida* cell death compared to the control *Candida* infection, with most of RHOE cells in the former appearing to be alive. Furthermore, the antifungal action of these derivatives was at least two-fold higher than the native drug and the hierarchy of activity was as follows: Nys7 > Nys5 > Nys1 (Fig. 3A). Subsequently, we demonstrated that these novel derivatives also exhibited low toxicity to human oral epithelium under infection conditions (Fig. 3B). In these experiments it was calculated that up to 4-fold more tissue keratinocytes were ‘live’ in the presence of compounds: Nys1 and Nys5 compared with Nystatin A₁. In the case of derivative Nys7, we calculated a 2-fold reduction in

toxicity. These data were in agreement with the cytotoxicity results on HaCaT cells, as we similarly found Nystatin A₁ to be the most toxic antifungal. For the novel derivatives at the concentration of 150 µg ml⁻¹, we found at least a three-fold decrease in toxicity to HaCaT cell line relative to native Nystatin A₁ (Fig. 8). There was no statistical difference between the toxicity of these derivatives ($P > 0.05$), confirming our earlier assumptions that the type of substituent at the amino group of Nystatin A₁ had little impact for toxicity reduction of new derivatives, and it was rather the substitution itself that mattered.

Interestingly, the antifungal efficacy results obtained from the infection model contrasted somewhat with the previously determined MICs from broth microdilution studies, with Nystatin A₁ demonstrating lower activity against *Candida* than the derivatives in the RHOE model. This effect may be associated with the high tendency of the polyene antibiotics to aggregate, which is crucial in their mode of action [21, 48]. As described for Amphotericin B, in aqueous solutions, polyenes exist as a mixture of monomers, water-soluble dimers/oligomers and/or water-insoluble larger aggregates and their relative proportions strongly depend on concentration. Bolard et al. [48] found, that a monomeric form of Amphotericin B, whilst active against fungal membranes, had no toxicity towards mammalian cells. Meanwhile, and in contrast to water-insoluble aggregates, which were not active against both types of cells, water-soluble oligomers characterised for both antifungal activity and host cell toxic effects. These reports may assist in the understanding of our results. It is believed that Nystatin A₁ has greater likelihood of undergoing different forms of aggregation (oligomers and larger coaggregates) than the new derivatives. This is because the predisposition to self-association may be hampered in the latter by the presence of a heavy substituent at the amino group of the molecule, and this was also previously observed for Amphotericin B derivatives [45]. Therefore, we hypothesise that at high concentrations, the water-insoluble aggregates form in the case of Nystatin A₁, but probably not for the derivatives, and this could decrease the total antifungal action of the former. Meanwhile, under the MICs test conditions, lower Nystatin A₁ concentrations were studied and therefore in these situations a greater extent of monomers and water-soluble oligomers could be formed resulting in lower MIC values (better antifungal activity *in vitro*).

Overall, it seems that the bioavailability of the novel derivatives with reduced propensity to aggregation (water-solubility), has been improved relative to Nystatin A₁, leading to enhanced antifungal action in infected tissues. However, it is difficult to ascertain this with certainty given the large size of the Nystatin A₁ molecule, the complexity of the research model (*Candida*-RHOE) and limited information on Nystatin A₁ aggregation process.

Additional interesting observations were made in the studies of tissue colonisation and invasion by *Candida*. Firstly, analysis showed that *C. albicans* ATCC 10231 extensively colonised the surface of the human oral epithelium and was able to invade the tissue to a high level (Fig. 5A). Similar to other authors [49, 50], we showed the presence of *Candida* biofilm on the RHOE surface and based on other studies involving clinical isolates of *C. albicans* [51, 52], we classified this strain as a ‘high invader’,

with an uniform pattern of invasion (Fig. 9). Our measurements of the biofilm thickness were likewise consistent with the earlier findings [53], in which the thickness of *Candida* biofilm under *in vitro* conditions was determined at between 25 μm and 450 μm . Whilst yeast cells were clearly detected within the tissue, hyphae were the predominant fungal elements penetrating all the RHOE layers, and this feature has also previously been noted [51, 52, 54]. Although, yeast forms were characterised to be actively non-invading cells, Jacobsen et al. [55] postulated that hyphae could facilitate the entry of yeast into tissue and under *in vivo* conditions these may contribute *Candida* dissemination into the bloodstream.

As a consequence of *Candida* RHOE infection, detachment of the epithelium from the basement membrane was evident, as were the occurrences of vacuolated spaces within the tissue structure, indicating damage. The same symptoms of epithelial disruption were found in the case of *C. albicans* SC5314 (ATCC MYA-2876) [25, 54] as well as in clinical isolates [51, 56]. Finally, CLSM analysis supported by the levels of LDH activity, providing a quantitative indicator of tissue cells damage. The results showed that the *Candida* were responsible for epithelium destruction after 24 h, as we recorded the highest LDH activity only in the presence of the fungus (Fig. 7).

Importantly, treatment of infected tissues with new polyene compounds successfully inhibited the *Candida* infection (Fig. 5C, D, E). Noteworthy, was the finding that the Nystatin A₁ derivatives were more effective in combating *Candida* tissue colonisation than the native Nystatin A₁, and this was confirmed by live/dead cell calculations. In addition, the presence of novel compounds resulted in thinner, less clustered and even somehow disrupted (in the case of Nys1) biofilm-like structures on tissue surfaces, compared to the native antibiotic. More specifically, we established that the *Candida* biofilm thickness under the effect of Nys5 and Nys7 derivatives was reduced by 29% and 36% in relation to the Nystatin A₁. Whereas, the compound Nys1 caused a 50% decrease in fungal biofilm formation, comparing with the parent drug (Fig. 6).

With respect to this, several authors [49, 50, 57] reported the resistance of *in vitro* *Candida* biofilms to antifungals, including Nystatin agent [58]. We also consider that the biofilm form of growth is less susceptible (than planktonic) to antifungal treatment, because we used high concentrations of compounds (150 $\mu\text{g ml}^{-1}$), and still observed a relatively thick *Candida* layer (50% that of untreated controls) after Nystatin treatment. However, the extent of drug diffusion may also be relevant to these findings [59]. Notwithstanding, novel derivatives exhibited a higher anti-biofilm effect. As we mentioned before, this result is most likely associated with improved water solubility of the later, in contrast to insoluble Nystatin A₁. Moreover, Chandra et al. [53] suggested that resistance of *Candida* biofilms to antifungals increases during biofilm maturation. We think it would be interesting to investigate the efficiency of novel compounds on different developmental *Candida* biofilm phases in the RHOE model, since in the present study we have analysed the effect of Nystatin A₁ and its derivatives on the early stages of *Candida* biofilm formation.

Furthermore, we found that *C. albicans* was unable to penetrate the oral epithelium after treatment with Nys5 and Nystatin A₁, whilst at the same time, moderate and low invasion levels were still seen for tissues after treatment with Nys1 and Nys7. It was particularly interesting to note that the nature of Nystatin modification appeared to influence the extent of *C. albicans* invasiveness, since complete prevention was found only in the case of Nys5 (*N*-succinimidyl derivative). We also detected a positive relationship between the MIC (IC50-C) for the derivatives and extent of *Candida* invasion.

Candida colonisation of the epithelium appeared less dependent on derivatisation, although it seemed that Nys1 (*N*-alkyl derivative) impacted differently on biofilm formation than the others, but this may have been associated with higher invasion level, since more fungal cells would have penetrated from the surface into the tissue. Nevertheless, the separation of epithelium from the base membrane was not found, as reported in the absence of polyene compounds. However, in terms of LDH activity, we demonstrated that Nystatin A₁ was 4-fold more toxic to RHOE than novel derivatives, with the latter resulting in statistically similar enzyme activity levels to those in the absence of *Candida* (Fig. 7).

In conclusion, the present study has examined the action of novel Nystatin A₁ derivatives (modified at the amino group) in an *in vitro* tissue model infected with *C. albicans* ATCC 10231. According to our knowledge, no efficiency/toxicity studies of polyene antibiotics in the *Candida*-RHOE model have previously been reported. The experiments showed that novel Nystatin derivatives were more effective in terms of antifungal activity, than the parent molecule. It is necessary to mention that these derivatives significantly inhibited *Candida* colonisation, including biofilm-like structure formation and highly reduced or completely prevented *Candida* invasion. We also showed, that these new polyenes were less toxic against keratinocyte cells, as well as the human oral epithelium compared with the natural Nystatin A₁. Although, broth microdilution derived MICs were not extrapolated to the tissue model, we have proposed a possible explanation for this. We have successfully applied a live/dead stain to calculate the ratio of live and dead *Candida* and tissue cells *in situ* and these results were comparable with histological observations of RHOE colonization and invasion by *C. albicans* and LDH activity measurements. Based on live/dead calculations we demonstrated that the hierarchy of antifungal activity under tissue conditions were: Nys7 > Nys5 > Nys1 > Nys, whilst the effect on the level of epithelium colonization and invasion by *Candida* seemed to be following: Nys7 ≥ Nys5 > Nys1 > Nys. Meanwhile, toxicity of the polyene antifungals assessed during viability studies decreased as follows: Nys > Nys7 > Nys5 ≥ Nys1 and similarly in terms of LDH activity level: Nys > Nys7 ≥ Nys5 ≥ Nys1.

We therefore report on the benefits of these novel Nystatin A₁ derivatives as alternatives to Nystatin A₁ as the former have greatly reduced toxicity to human epithelial cells with an associated high antifungal activity. Further research into the mechanism of this selective toxicity exhibited by the new Nystatin A₁ derivatives is required and such studies are currently in progress.

Acknowledgements

We would like to thank Mrs Kath Allsopp for processing and sectioning tissue samples. We are also grateful to Mr Marc Isaacs for help with confocal scanning laser microscopy. The project was financed by the National Science Centre (Poland) based on the grant no. DEC-2011/01/N/NZ1/05269 (PRELUDIUM: pre-doctoral grant).

References

1. Farah CS, Ashman RB, Challacombe SJ (2000) Oral candidosis. *Clin Dermatol* 18:553-62
2. Joint United Nations Programme on HIV/AIDS (UNAIDS) and World Health Organization (WHO) (2009) AIDS epidemic update: November 2009, Geneva, Switzerland
3. Petersen PE (2008) Oral cancer prevention and control – The approach of the World Health Organization. *Oral Oncol*. doi:10.1016/j.oraloncology.2008.05.023
4. World Health Organization (2013) Diabetes Programme: fact sheet N°312. <http://www.who.int/diabetes/en/>. Updated March 2013, Geneva, Switzerland
5. Mane A, Gaikwad S, Bembalkar S, Risbud A (2012) Increased expression of virulence attributes in oral *Candida albicans* isolates from human immunodeficiency virus-positive individuals. *J Med Microbiol* 61:285-290. doi: 10.1099/jmm.0.036269-0.
6. Davies AN, Brailsford SR, Beighton D (2006) Oral candidosis in patients with advanced cancer. *Oral Oncol* 42:698-702
7. Soysa NS, Samaranayake LP, Ellepola ANB (2005) Diabetes mellitus as a contributory factor in oral candidosis. *Diabet Med* 23:455-459
8. Farah CS, Lynch N, McCullough MJ (2010) Oral fungal infections: an update for the general practitioner. *Aust Dent J* 55: 48-54. doi: 10.1111/j.1834-7819.2010.01198.x.
9. Krishnan PA (2012) Fungal infections of the oral mucosa. *Indian J Dent Res* 23:650-659. doi: 10.4103/0970-9290.107384.
10. Zhu W, Filler SG (2010) Interactions of *Candida albicans* with epithelial cells. *Cell Microbiol* 12:273-282. doi: 10.1111/j.1462-5822.2009.01412.x.
11. Mayer FL, Wilson D, Hube B (2013) *Candida albicans* pathogenicity mechanisms. *Virulence* 4:119-128. doi: 10.4161/viru.22913.
12. Samaranayake LP, Keung Leung W, Jin L (2009) Oral mucosal fungal infections. *Periodontol* 2000 49:39-59. doi: 10.1111/j.1600-0757.2008.00291.x.
13. Williams D, Lewis M (2011) Pathogenesis and treatment of oral candidosis. *J Oral Microbiol* 3. doi: 10.3402/jom.v3i0.5771.
14. Ellepola ANB, Samaranayake LP (2000) Oral candidal infections and antimycotics. *Crit Rev Oral Biol Med* 11:172-198
15. Lewis RE (2011) Current concepts in antifungal pharmacology. *Mayo Clin Proc* 86:805-817

16. Wakieć R, Prasad R, Morschhäuser J, Barchiesi F, Borowski E, Milewski S (2007) Voriconazole and multidrug resistance in *Candida albicans*. *Mycoses* 50:109-115
17. Zotchev SB (2003) Polyene macrolide antibiotics and their applications in human therapy. *Curr Med Chem* 10:211-223
18. Pierce CG, Lopez-Ribot JL (2013) Candidiasis drug discovery and development: new approaches targeting virulence for discovering and identifying new drugs. *Expert Opin Drug Discov*. doi:10.1517/17460441.2013.807245
19. Chéron M, Cybulska B, Mazerski J, Grzybowska J, Czerwiński A, Borowski E (1988) Quantitative structure-activity relationships in amphotericin B derivatives. *Biochem Pharmacol* 37:827-836
20. Baginski M, Czub J (2009) Amphotericin B and its new derivatives – mode of action. *Curr Drug Metab* 10:459-469
21. Volmer AA, Szpilman AM, Carreira EM (2010) Synthesis and biological evaluation of amphotericin B derivatives. *Nat Prod Rep* 27:1329-1349. doi: 10.1039/b820743g.
22. Paquet V, Volmer AA, Carreira EM (2008) Synthesis and *in vitro* biological properties of novel cationic derivatives of amphotericin B. *Chemistry* 14:2465-2481. doi: 10.1002/chem.200701237.
23. Borowski E, Salewska N, Boros-Majewska J, Milewska M, Wysocka M, Milewski S, Składanowski A, Treder A, Sadowska E, Łacka I (2013) Semisynthetic derivatives of Nystatin A₁. PCT/EP2013/054621; WO 2013/132014 A1 (12 September 2013)
24. Schaller M, Schäfer W, Korting HC, Hube B (1998) Differential expression of secreted aspartyl proteinases in a model of human oral candidosis and in patient samples from the oral cavity. *Mol Microbiol* 29:605-615
25. Schaller M, Zakikhany K, Naglik JR, Weindl G, Hube B (2006) Models of oral and vaginal candidiasis based on *in vitro* reconstituted human epithelia. *Nat Protoc* 1:2767-2773
26. Falkowski L, Kowszyk-Gindifer Z, Plóciennik Z, Zieliński J, Dahlig H, Golik J, Jakobs E, Kołodziejczyk P, Bylec E, Roślik-Kamińska D, Wagner W, Pawlak J, Borowski E (1980) Salts of *N*-glycosyl derivatives of polyene macrolides, especially *N*-methylglucamine salts as well as the method of their preparation. Patent USA 4195172 A
27. The National Committee for Clinical and Laboratory Standards (2002) Reference Method for Broth Dilution Antifungal Susceptibility Testing of Yeasts; Approved Standard-Second Edition M27-A2. NCCLS, 2002, Wayne, PA, USA
28. Ōmura S (1984) *Macrolide Antibiotics: Chemistry, Biology, and Practice*. Academic Press, Orlando, Florida
29. Larson JL, Wallace TL, Tyl RW, Marr MC, Mayers CB, Cossum PA (2000) The reproductive and development toxicity of the antifungal drug Nyotran (liposomal Nystatin) in rats and rabbits. *Toxicol Sci* 53:421-429
30. Semis R, Polacheck I, Segal E (2010) Nystatin-intralipid preparation: characterization and *in vitro* activity against yeasts and molds. *Mycopathologia* 169:333-341



31. Arian S, Rex JH (2001) Nystatin LF (Aronex/Abbott) *Curr Opin Investig Drugs* 2:488-495
32. Barrat G, Bretagne S (2007) Optimizing efficacy of Amphotericin B through nanomodification. *Int J Nanomedicine* 2:301-313
33. Semis R, Kagan S, Berdicevsky I, Polacheck I, Segal E (2013) Mechanism of activity and toxicity of Nystatin-intralipid. *Med Mycol* 51:422-431. doi: 10.3109/13693786.2012.731712.
34. Semis E, Nili SS, Munitz A, Zaslavsky Z, Polacheck I, Segal E (2012) Pharmacokinetics, tissue distribution and immunomodulatory effect of intralipid formulation of Nystatin in mice. *J Antimicrob Chemother* 67:1716-1721. doi: 10.1093/jac/dks117.
35. Brautaset T, Sletta H, Nedal A, Borgos SEF et al (2008) Improved antifungal polyene macrolides via engineering of the Nystatin biosynthetic genes in *Streptomyces noursei*. *Chem Biol* 15:1198-1206. doi: 10.1016/j.chembiol.2008.08.009.
36. Bruheim P, Borgos SE, Tsan P, Stella H, Ellingsen TE, Lancelin JM, Zotchev SB (2004) Chemical diversity of polyene macrolides produced by *Streptomyces noursei* ATCC 11455 and recombinant strain ERD44 with genetically altered polyketide synthase NysC. *Antimicrob Agents Chemother* 48:4120-4129
37. Caffrey P, Aparicio JF, Malpartida F, Zotchev SB (2008) Biosynthesis engineering of polyene macrolides towards generation of improved antifungal and antiparasitic agents. *Curr Top Med Chem* 8:639-653
38. Falk R, Domb AJ, Polacheck I (1999) A novel injectable water-soluble amphotericin B-arabinogalactan conjugate. *Antimicrob Agents Chemother* 43:1975-1981
39. Szlinder-Richert J, Mazerski J, Cybulska B, Grzybowska J, Borowski E (2001) MFAME, N-methyl-N-D-fructosyl amphotericin B methyl ester, a new amphotericin B derivative of low toxicity: relationship between self-association and effects on red blood cells. *Biochim Biophys Acta* 1528:15-24
40. Paquet V, Carreira EM (2006) Significant improvement of antifungal activity of polyene macrolides by bisalkylation of the mycosamine. *Org Lett* 8:1807-1809
41. Lewis RE, Viale P (2012) Update on amphotericin B pharmacology and dosing for common systemic mycoses. *Curr Fungal Infect Rep* 6:349-357. doi:10.1007/s12281-012-0107-9.
42. Moharamzadeh K, Colley H, Murdoch C, Haernden V, Chai WL, Brook IM, Thornhill MH, MacNeil S (2012) Tissue-engineered oral mucosa. *J Dent Res* 91:642-50. doi: 10.1177/0022034511435702.
43. Carrillo-Muñoz AJ, Quindós G, Tur C, Ruesga MT, Miranda Y, del Valle O, Cossum PA, Wallace TL (1999) In-vitro antifungal activity of liposomal nystatin in comparison with nystatin, amphotericin B cholesteryl sulphate, liposomal amphotericin B, amphotericin B lipid complex, amphotericin B desoxycholate, fluconazole and itraconazole. *J Antimicrob Chemother* 44:397-401

44. Arikan S, Ostrosky-Zeichner L, Lozano-Chiu M, Paetznick V, Gordon D, Wallace T, Rex JH (2002) In vitro activity of nystatin compared with those of liposomal nystatin, amphotericin B, and fluconazole against clinical *Candida* isolates. *J Clin Microbiol* 40:1406-1412
45. Borowski E (2000) Novel approaches in the rational design of antifungal agents of low toxicity. *Farmacologia* 55:206-208
46. Slisz M, Cybulska B, Mazerski J, Grzybowska J, Borowski E (2004) Studies of the effects of antifungal cationic derivatives of amphotericin B on human erythrocytes. *J Antibiot (Tokyo)* 57:669-678
47. Martin R, Wächtler B, Schaller M, Wilson D, Hube B (2011) Host-pathogen interactions and virulence-associated genes during *Candida albicans* oral infections. *Int J Med Microbiol* 301:417-422. doi: 10.1016/j.ijmm.2011.04.009.
48. Legrand P, Romero EA, Cohen BE, Bolard J (1992) Effects of aggregation and solvent on the toxicity of amphotericin B to human erythrocytes. *Antimicrob Agents Chemother* 36:2518-2522
49. Seneviratne SJ, Jin L, Samaranayake LP (2008) Biofilm lifestyle of *Candida*: a mini review. *Oral Dis* 14:582-590. doi: 10.1111/j.1601-0825.2007.01424.x.
50. Williams DW, Kuriyama T, Silva S, Malic S, Lewis MAO (2011) *Candida* biofilms and oral candidosis: treatment and prevention. *Periodontol* 2000 55:250-265. doi: 10.1111/j.1600-0757.2009.00338.x.
51. Bartie KL, Williams DW, Wilson MJ, Potts AJC, Lewis MAO (2004) Differential invasion of *Candida albicans* isolates in an *in vitro* model of oral candidosis. *Oral Microbiol Immunol* 19:293-296
52. Malic S, Hill KE, Ralphs JR, Hayes A, Thomas DW, Potts AJ, Williams DW (2007) Characterization of *Candida albicans* infection of an *in vitro* oral epithelial model using confocal laser scanning microscopy. *Oral Microbiol Immunol* 22:188-194
53. Chandra J, Kuhn DM, Mukherjee PK, Hoyer LL, McCormick T, Ghannoum MA, (2001) Biofilm formation by the fungal pathogen *Candida albicans*: development, architecture, and drug resistance. *J Bacteriol* 183: 5385-5394
54. Zakikhany K, Naglik JR, Schmidt-Westhausen A, Holland G, Schaller M, Hube B (2007) In vivo transcript profiling of *Candida albicans* identifies a gene essential for interepithelial dissemination. *Cell Microbiol* 9:2938-2954
55. Jacobsen ID, Wilson D, Wächtler B, Brunke S, Naglik JR, Hube B (2012) *Candida albicans* dimorphism as a therapeutic target. *Expert Rev Anti Infect Ther* 10:85-93. doi: 10.1586/eri.11.152.
56. Silva S, Henriques M, Hayes A, Oliveira R, Azeredo J, Williams DW (2011) *Candida glabrata* and *Candida albicans* co-infection of an *in vitro* oral epithelium. *J Oral Pathol Med* 40:421-427
57. Baillie GS, Douglas LJ (1998) Effect of growth rate on resistance of *Candida albicans* biofilms to antifungal agents. *Antimicrob Agents Chemother* 42:1900-1905

58. Chandra J, Mukherjee PK, Leidich SD, Faddoul FF, Hoyer LL, Douglas LJ, Ghannoum MA (2001) Antifungal resistance of candidal biofilms formed on denture acrylic in vitro. *J Dent Res* 80:903-908
59. Samaranayake YH, Ye J, Yau JYY, Cheung BPK, Samaranayake LP (2005) In vitro method to study antifungal perfusion in *Candida* biofilms. *J Clin Microbiol* 43:818-825. doi:10.1128/JCM.43.2.818-825.2005
60. Kuriyama T, Williams DW, Bagg J, Coulter WA, Ready D, Lewis MAO (2005) *In vitro* susceptibility of oral *Candida* to seven antifungal agents. *Oral Microbiol Immunol* 20:349-353

Figure legends

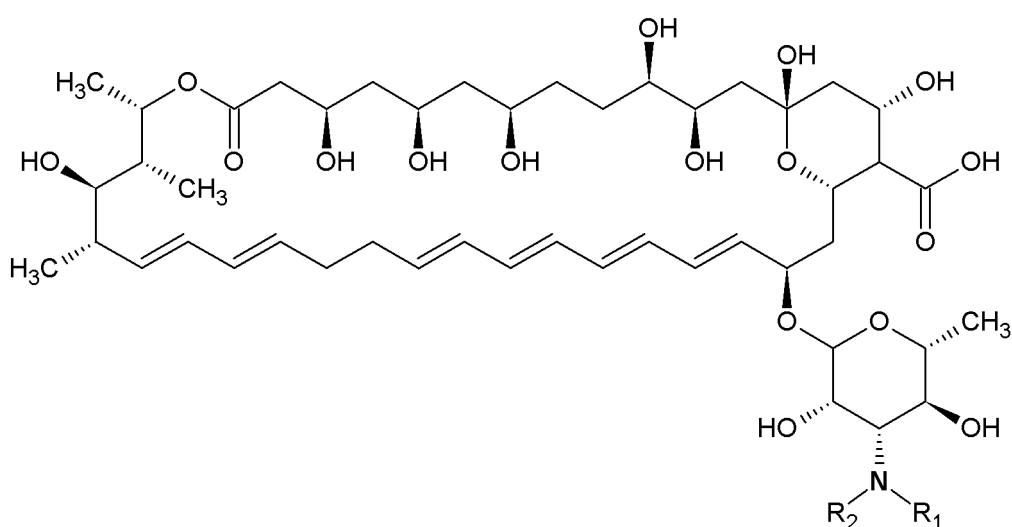


Figure 1. The chemical structure of Nystatin A₁ and tested derivatives.

Nys: R₁=R₂=H; **Nys1:** R₁=methyl, R₂=methyl; **Nys2:** R₁=H, R₂=2-(*N*-methylamino)-2-methylpropionyl; **Nys3:** R₁=H, R₂=fructosyl; **Nys4:** R₁=H, R₂=*N*'-3-(*N*'',*N*''-dimethylamino)propylsuccinimidyl; **Nys5:** R₁=H, R₂=*N*'-2-(piperidin-1-yl)ethylsuccinimidyl; **Nys6:** R₁=3-[2-(*N,N*-diethylamino)ethyl]thioureidyl; **Nys7:** R₁=H, R₂=3-[3-(*N,N*-dimethylamino)propyl]thioureidyl; **Nys8:** R₁=H, R₂=3-[2-(*N,N*-dimethylamino)ethyl]thioureidyl.

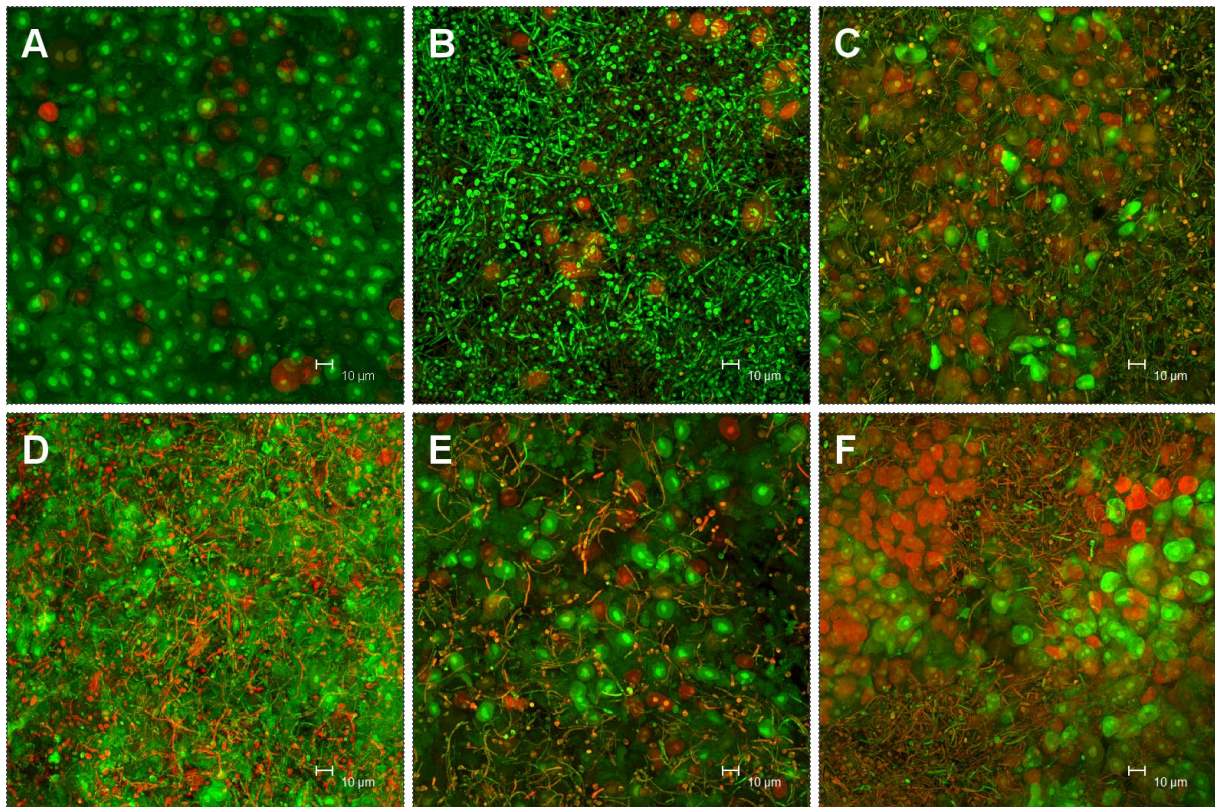


Figure 2. The viability of *Candida* and epithelial cells as detected by confocal scanning laser microscopy. Tissue devoid of fungal cells (A) and after the infection (B-F) were imaged using a live/dead assay. RHOE tissues were inoculated for 6 h with *Candida albicans* ATCC 10231 strain and treated with the solvent alone (B-1% v/v DMSO) or 150 $\mu\text{g ml}^{-1}$ of antifungals for 16 h (C-Nys, D-Nys1, E-Nys5, F-Nys7). Green cells were stained with Syto9, while orange/red with both Syto9 and propidium iodide.

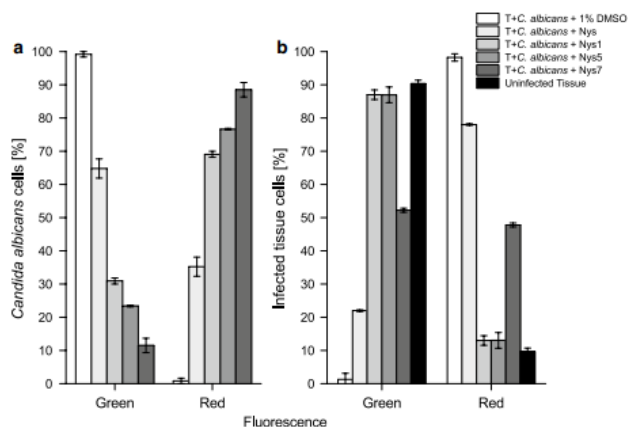


Figure 3. The ratio of green and red fluorescence of *Candida albicans* (A) and epithelial cells (B) after RHOE infection and treatment with antifungal compounds or solvent alone (1% v/v DMSO), based on CLSM images. Areas of green and red fluorescence for each cell type in a single image were summed, taken as a total and the percent of fluorescence was calculated separately for *Candida* and epithelial cells. Results for uninfected tissue control were also included (B). Fluorescence measurements were made using ImageJ 1.46r software. Diagrams illustrate the mean from three independent images.

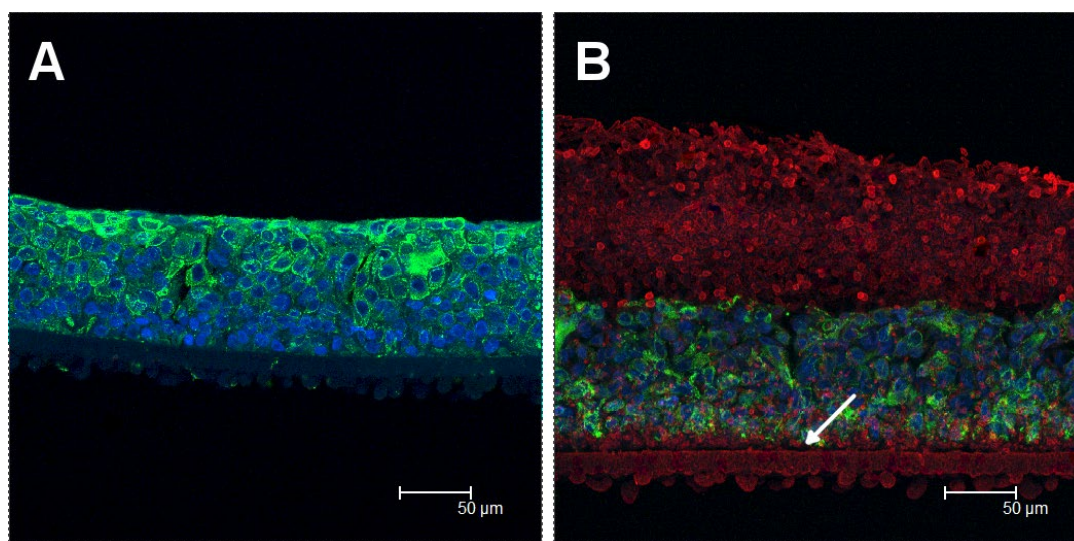


Figure 4. Confocal scanning laser microscopy of uninfected control of reconstituted human oral epithelium (A) and after infecting with *Candida albicans* ATCC 10231 strain (B). Tissues were fixed, sectioned and subjected to immunostaining. Keratinocytes were detected with a mouse monoclonal IgG pan-cytokeratin primary antibody and visualized with an Alexa Fluor 488 goat anti-mouse IgG (green). A Hoechst 33258 dye was used to localize epithelial cells nuclei (blue). *Candida* cells were differentiated by concanavalin A lectin conjugated with Alexa Fluor 594 (red). An arrow indicates keratinocytes detachment from the membrane base.

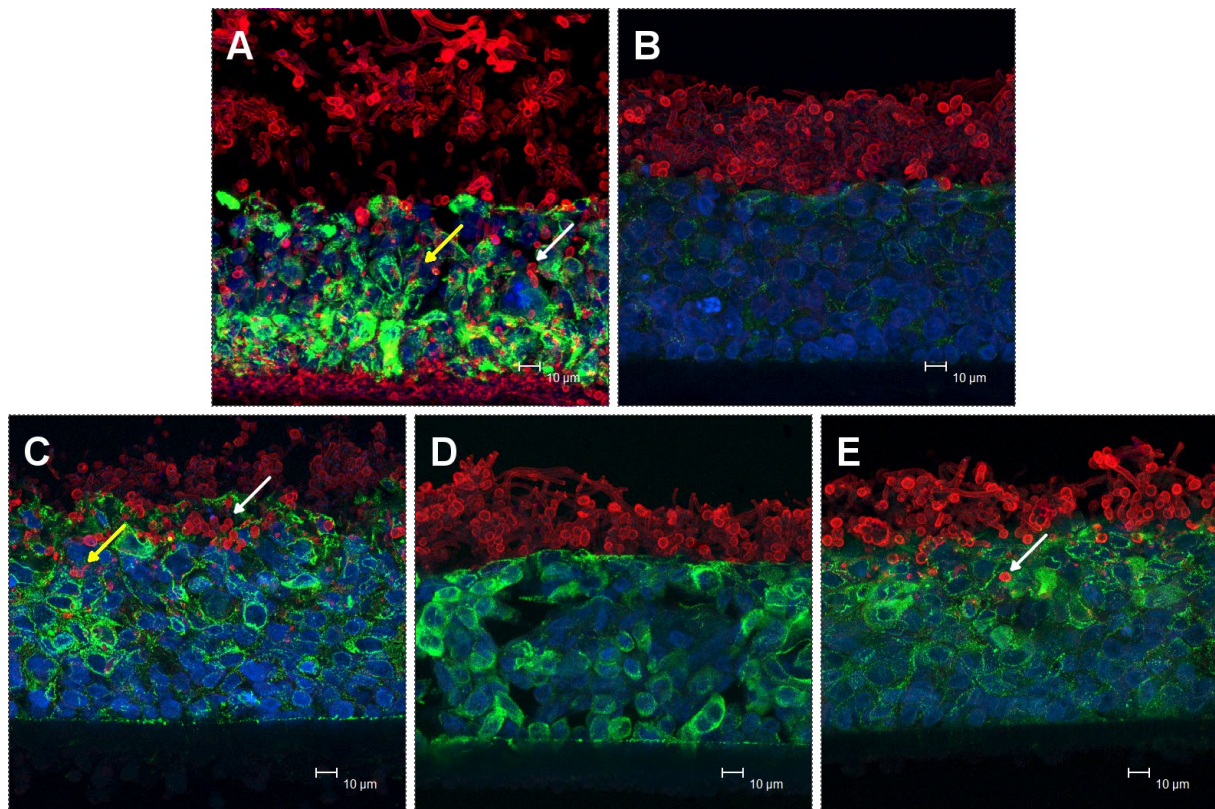


Figure 5. Colonization and invasion of oral epithelium by *Candida albicans* illustrated by CLSM, in the absence (A) or presence (B-E) of antifungals. (A) Extensive colonization and invasion with 1% (v/v) DMSO; (B) moderate colonization and no invasion with Nys; (C) low colonization and moderate invasion with Nys1; (D) low colonization and no invasion with Nys5; (E) low colonization and low invasion with Nys7. Legend: +++, extensive; ++, moderate; +, low. RHOE tissues were prepared according to standard histological techniques and proceed with immunostaining (read *legend of Figure 4*). Keratinocytes were stained in green, nuclei content were blue, while *Candida* cells were shown as red. Arrows indicate *Candida albicans* hyphae (yellow) and yeast cells (white) penetrating tissues.

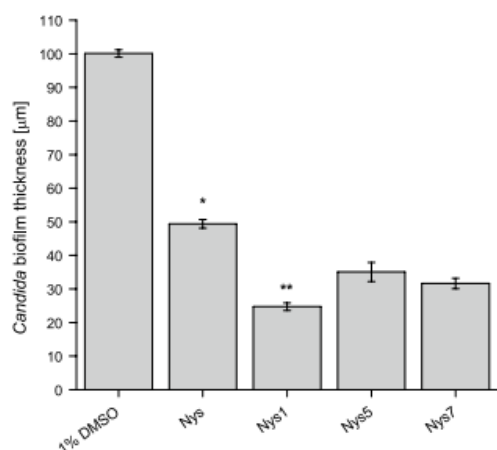


Figure 6. Thickness of the biofilm formed by *Candida albicans* on the oral epithelium surface after treatment with solvent (1% v/v DMSO) or polyene antifungals. Calculations were made based on CLSM images of immunostained RHOE sections with the use of ImageJ 1.46r software. Diagram represents the mean of three independent images. * Thickness of *Candida* layer was not statistically different in case of derivatives Nys5 and Nys7 ($P > 0.05$), according to one-way analysis of variance (ANOVA), followed by Tukey multiple comparisons test.

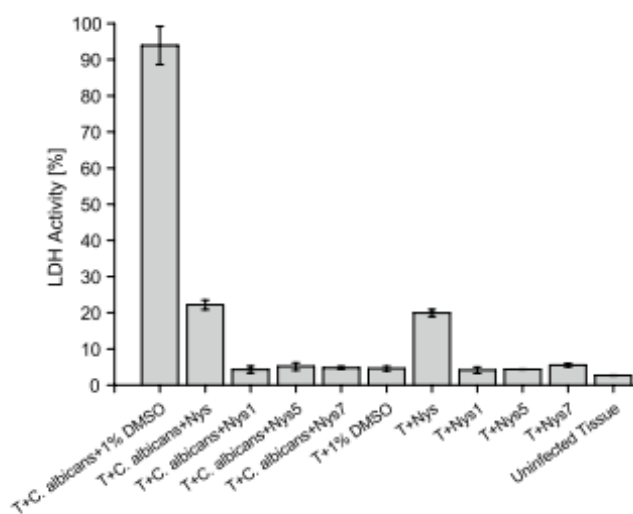


Figure 7. Lactate dehydrogenase (LDH) activity measured in the culture medium collected after RHOE infection with *Candida albicans* and exposure to antifungal compounds or solvent alone (1% v/v DMSO). LDH activity from uninfected RHOE tissues after treatment with tested agents or 1% DMSO, as well as from uninfected tissue controls were presented. T- means RHOE tissue. * LDH activity influenced by Nys was not statistically different for infected and uninfected oral epithelium ($P > 0.05$). ** LDH activity in case of new derivatives was not statistically different for infected and uninfected oral epithelium and for uninfected oral epithelium with 1% DMSO ($P > 0.05$). One-way analysis of variance (ANOVA), followed by Tukey multiple comparisons test was used.



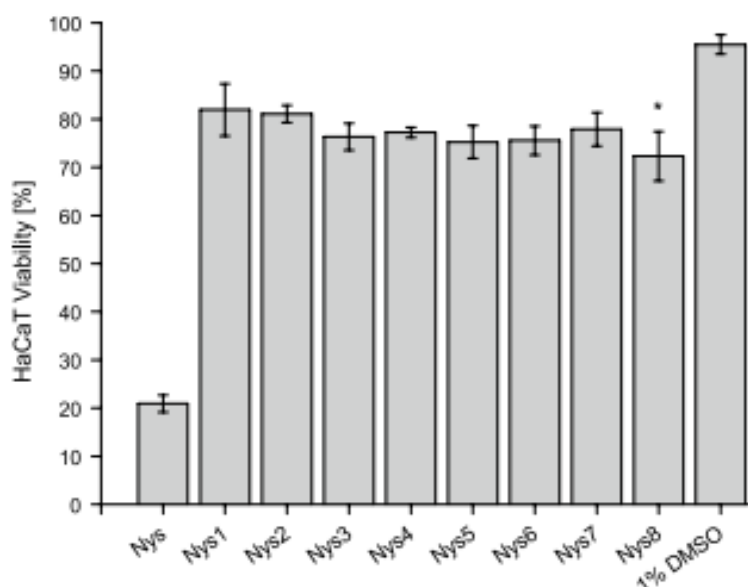


Figure 8. *In vitro* viability of human keratinocyte cell line (HaCaT) in the presence of $150 \mu\text{g ml}^{-1}$ of antifungal compounds dissolved in DMSO and the control of solvent alone (1% v/v DMSO), measured after 3 days of incubation by using the CCK-8 assay. The percentage of viable cells was calculated based on optical density values (OD450) in relation to the drug free control. * HaCaT viability was not statistically different ($P > 0.05$) in the presence of tested derivatives. One way analysis of variance (ANOVA), supported by Tukey multiple comparisons test was applied.

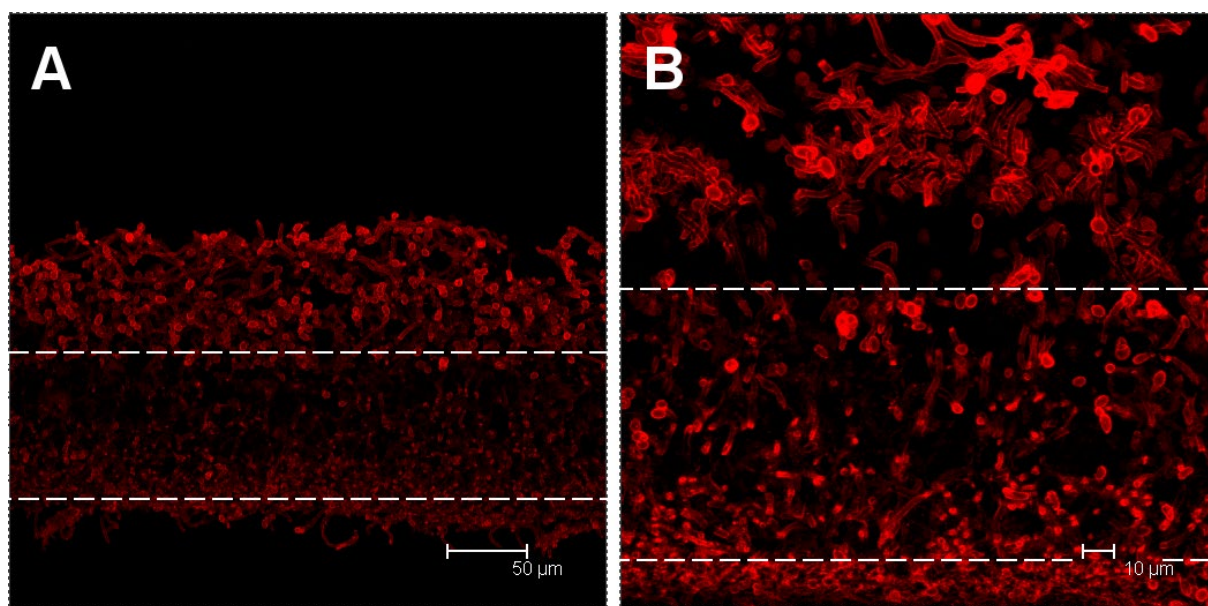


Figure 9. Uniform pattern of oral epithelium invasion by *Candida albicans* cells, labelled with concanavalin A lectin conjugated with Alexa Fluor 594 (red), at low (A) and high (B) magnification, imaged by CLSM. Dashed lines symbolize the RHOE tissue.

Tables

Table 1 Antifungal activity of Nystatin A₁ and *N*-substituted derivatives against *Candida albicans* ATCC 10231 as determined by broth microdilution

Compound	MIC ($\mu\text{g ml}^{-1}$)	IC ₅₀ -C ($\mu\text{g ml}^{-1}$)
Nys *	0.5	0.21
<i>N</i>-alkyl derivatives		
Nys1	4	2.81
<i>N</i>-aminoacyl derivatives		
Nys2	4	2.61
<i>N</i>-fructosyl derivatives		
Nys3	8	3.06
<i>N</i>-succinimidyl derivatives		
Nys4	8	3.89
Nys5	2	1.19
Thioureidyl derivatives		
Nys6	8	4.65
Nys7	4	2.81
Nys8	4	2.35

* Breakpoint for resistance to Nystatin A₁: MIC \geq 16 ($\mu\text{g ml}^{-1}$) [60]

Table 2 Cytotoxicity of Nystatin A₁ and *N*-substituted derivatives to HaCaT cell line defined by using the Cell Counting Kit-8

Compound	IC ₅₀ -H ($\mu\text{g ml}^{-1}$)
Nys	50.82
<i>N</i>-alkyl derivatives	
Nys1	>300

<i>N</i>-aminoacyl derivatives	
Nys2	>300
<i>N</i>-fructosyl derivatives	
Nys3	>300
<i>N</i>-succinimidyl derivatives	
Nys4	>300
Nys5	>300
Thioureidyl derivatives	
Nys6	>300
Nys7	>300
Nys8	>300

Table 3 *Candida albicans* colonisation and invasion of reconstituted human oral epithelium influenced by Nystatin A₁ and *N*-substituted derivatives and evaluated by confocal laser scanning microscopy

Sample	Colonisation	Invasion
1% DMSO	+++	+++
Nys	++	none
Nys1	+	++
Nys5	+	none
Nys7	+	+

Legend: +++, extensive; ++, moderate; +, low.